Robust and transparent smooth amphi-repellent coating with physical and chemical self-cleaning properties

Panagiotis N. Manoudis[1], Ioannis Zuburtikudis[2], Hadil Abu Khalifeh[2] and Ioannis Karapanagiotis[3*]

[1]Lysis Consulting P.C., 55534 Thessaloniki, Greece

[2]Department of Chemical Engineering, Abu Dhabi University (ADU), P.O. Box 59911, Abu Dhabi, United Arab Emirates

[3]Department of Chemistry, Aristotle University of Thessaloniki, 54124 Thessaloniki, Greece

*karapana@chem.auth.gr

Abstract

Smooth amphiphobic and amphi-repellent surfaces have attracted attention, because their ability to repel liquids possessing a broad range of surface tensions offers the potential to be used for the protection of various surfaces, including glass, keeping them dust- and dirt-free through the physical self-cleaning mechanism. We report the production of a coating which combines liquid amphi-repellency (i.e. physical self-cleaning) with phtotocatalytic activity (i.e. chemical self-cleaning). Consequently, the produced coating has an enhanced self-cleaning capacity which originates from two different (physical and chemical) mechanisms. Since the coating is designed for glass protection attention focuses on maintaining optical transparency of glass. The coating consists of a fluorosilane (1H,1H,2H,2H-Perfluorooctyltriethoxysilane) and titanium oxide (TiO_2) nanoparticles. The effects of (i) the number of dip coating cycles which were applied to treat glass and (ii) the concentration of TiO_2 nanoparticles on optical transparency, wetting properties (i.e. physical liquid repellency) and photocatalytic activity are investigated. A coating prepared using two coating cycles and 0.25% w/w TiO_2 NPs was selected, as it combines the three aforementioned properties. The selected coating

shows very good mechanical stability against abrasion, resistance to degradation effects induced by the UV radiation, chemical stability and stain resistance and anti-smudge performance.

Keywords: *amphiphobic; omniphobic; liquid-repellent, photocatalytic; fluorosilane;* TiO_2

1. Introduction

Glass is a versatile material, used for example in windows, photovoltaics, vehicles and aircrafts, building façades and roofs, to name a few applications. The most useful property of glass is its transparency in visible light which, however, is affected and deteriorated by dirt and dust, as these contaminants do not allow visible light to pass through [1]. Dirt particles, derived from various natural sources (animals and plants) and anthropogenic activities (e.g. industrial and vehicle emissions and building materials) are carried by rain or wind and can become adhered to glass surfaces. Dust is less of a concern, because usually it can be washed easily away [1]. However, in certain areas, which suffer from desert storms and droughts, glass contamination by dust is a major issue which increases the frequency and therefore the cost of glass cleaning, particularly for hard-to-access facades and building overhangs [2].

Dust of atmospheric air is derived from natural phenomena (e.g. desert storms and volcanic eruptions) and anthropogenic activities (e.g. industrial and vehicle emissions) [3]. Various regions around the globe are major natural dust sources with the Sahara Desert being the major contributor to the global dust budget [4,5]. Other important regions of dust sources are located in America, Asia, Australia and Southern Africa [3-5]. It should be stressed that glass contamination by dust is not limited to these areas, as desert dust is easily transported to very long distances [6].

Different mitigation strategies for tackling the dirt and dust soiling problem on glass have been devised [7], as summarized in Table 1. Transparent, superhydrophilic coatings, with a contact angle of water (CA_W) drops close to 0°, can be deposited on glass inducing a physical self-cleaning mechanism, as dirt and dust are washed away by sheets of water which are formed by coalesced

rainwater drops [1]. Following this scenario, various materials such as superhydrophilic copolymers [8], nanocomposites [9] and bionic polymers [10] have been synthesized to produce self-cleaning coated glass.

Chemical self-cleaning is another strategy to maintain glass surfaces free of dirt. This strategy is based on the photocatalytic activity of semiconducting materials which is activated in the presence of the UV radiation and leads to the chemical decomposition of organic pollutants. The most prominent example of photocatalytic materials is titanium dioxide (TiO_2). Cleaning is achieved by the synergistic effects of the photocatalytic decomposition of pollutants and the photoinduced superhydrophilicity [11-13]. Photocatalysis leads to the decomposition of mainly organic pollutants, whereas mineralized residues and inorganic contaminants are washed away from the superhydrophilic surface by sheets of water [14]. Following this strategy, TiO_2 nanoparticles embedded in organic [15,16] and organosilicon, hybrid [17] matrices were deposited on glass which showed self-cleaning ability, combined with some other useful properties such as, for instance, antifogging and antifouling. Fewer in number are the research papers which produced self-cleaning coated glass using other photocatalytic materials other than TiO_2 e.g. zinc oxide, ZnO [18].

Following a different approach, the opposite wettability state of superhydrophilicity, which is superhydrophobicity, has been extensively investigated as a possible route to keep outdoor surfaces clean i.e. dust- and dirt-free. A water drop on a superhydrophobic ($CA_W > 150°$ and contact angle hysteresis, $CAH_W < 10°$) surface rolls off easily, removing any contaminant, thus leaving the surface clean [19]. This is a physical self-cleaning mechanism that originates from the non-wetting properties of textured superhydrophobic surfaces. Superhydrophobic coatings on glass were produced using various polymer blends (e.g. [20-22]) and composites of polymers and nanoparticles including, for instance silica (SiO_2) [23], alumina (Al_2O_3) [24], vanadium dioxide (VO_2) [25] and polytetrafluoroethylene (PTFE) nanoparticles [26]. However, textured surfaces suffer usually from poor mechanical durability, as their micro-/nano-hierarchical structures can be damaged, sometimes even under weakly applied loads. Hence, despite the huge investment in relative research, lotus-like

surfaces are still rarely seen in real-world applications [27]. Moreover, organic pollutants tend to adhere to superhydrophobic textured surfaces, as they are trapped within the morphological asperities, deteriorating the dewetting properties and the self-cleaning performance of the surfaces [28,29]. Finally, transition from the Cassie−Baxter [30] to the Wenzel [31] state is often observed on textured superhydrophobic [32,33] or superamphiphobic [34,35] surfaces, resulting on pinned drops which apparently cannot act as cleaning carriers. All these obstacles plague the practical applications of textured surfaces.

The combination of superhydrophobicity with photocatalysis was investigated as a potential strategy for tackling the aforementioned disadvantages of the textured superhydrophobic materials, by promoting their cleaning efficacy through chemical agents. However, the production of textured superhydrophobic coatings with photocatalytic properties is not easy, as upon exposure to the natural UV light, a wettability transition to superhydrophilicity is induced [36,37]. Hence, only few studies achieved to produce nanocomposite coatings of polymer matrices and TiO_2, which combined physical (through superhydrophobicity) and chemical (through photocatalysis) self-cleaning [38-43]. The strategy was followed to coat glass [41-43], but high transparency of coated-glass by visible light was only scarcely reported. For example, high transparency was achieved on glass which was coated by a superhydrophobic and photocatalytic composite material of polydimethylsiloxane (PDMS) and TiO_2 [43]. Another nanocomposite of polytetrafluoroethylene (PTFE) and TiO_2 showed high transparency, but this was used to coat quartz and not glass [38].

Slippery liquid-infused porous surfaces (SLIPS) have been introduced as an alternative approach [44-47] to address the drawbacks of solid textured superhydrophobic surfaces which were described above e.g. poor mechanical durability. The idea is to cover micro/nanoporous structures with a low surface-tension lubricant, which is immiscible with water. The standard physical self-cleaning scenario is realized on SLIPS by water drops which slide off easily [48]. However, SLIPS have some important drawbacks including the degradation, leakage, and vaporization of the lubricant over time and research to address these issues is still undertaken [49].

Fluorinated coatings, with exceptional repellency against low surface tension, non-polar liquids, have attracted attention as an alternative strategy for the protection of glass. The surfaces of these coatings are smooth i.e. non-textured. Because of the high fluorine content, drops of non-polar (contaminants) liquids do not stick on the coating surface, but they roll off easily, corresponding to low CAH (typically, <10°). Moreover, as described below, some methods achieved to report considerable repellency even for water drops i.e. low CAH_W. Consequently, the coating surface is not contaminated and is kept clean. With this strategy, several of disadvantages of the textured surfaces, described above, are addressed. For example, as the surfaces of the fluorinated coatings are smooth, they show high durability and transmittance in visible light. A variety of fluorinated polymers were used to coat glass and tested, as it is briefly summarised below.

In their pioneering work, Urata et al. produced several mixtures of perfluoroalkylsilanes with a range of different perfluoroalkyl groups and tetramethoxysilane [50]. CAH of non-polar liquids was <5° whereas the corresponding values for water drops (CAH_W) was on the order of 10°. The dynamic dewetting coatings showed chemical and thermal durability [50]. Jiang et al. synthesised and characterised a number of fluorinated polymers with short perfluorobutyl side chains which however resulted in relatively high CAH_W whereas the transmittance of visible light was not measured [51]. Boban et al. produced a transparent and durable amphiphobic coating composed of a fluorinated polyurethane and fluorodecyl polyhedral oligomeric silsesquioxane which gave CAHs of various liquids <15° [52]. Gao et al. used two kinds of siloxanes which were cross-linked to form a transparent coating on various substrates, including glass [53]. Attention focused on the anti-graffiti properties of the coating which gave low and high sliding angles for drops of non-polar liquids and water, respectively [53]. Psarski et al. performed a comparative study on the wettability and adhesion of coatings which were produced using a homologous series of fluoroalkyl silanes (FAS) and were deposited on silicon and glass following two vapor phase deposition techniques [54]. The reported CAHw on coated glass was on the order of 20° [54]. Liu et al. applied poly(dimethylsiloxane) (PDMS) on glass through a one-step grafting-from approach [55]. The layer of the covalently attached

PDMS brushes showed excellent durability, transmittance to visible light and amphiphobicity as the CAHs of various liquid drops, including CAH_W, were <5° [55]. In another study, perfluoropolyether chains were grafted on glass which obtained good stain resistance whereas transmittance in visible light was maintained [56]. CAHs varied from 12° to 60° for a large variety of liquid drops corresponding to very low (e.g. alkanes) and high (e.g. water) surface tensions [56]. Transparent coatings on glass were fabricated by Mayoussi et al. using five perfluoroalkyl methacrylates [48]. Two coatings showed very good repellency towards various liquids (including water) with different polarities, as evidenced by the corresponding low CAH (<5°). The self-cleaning and anti-graffiti ability of the coatings were shown [48].

In the present study the production of a transparent and robust coating, which combines physical and chemical self-cleaning properties, is reported. This is achieved by embedding carefully TiO_2 NPs into an amphiphobic fluorosilane of exceptional repellency i.e. low CAH. The coating is designed for glass protection. To the best of our knowledge this is the first attempt to combine the photocatalytic activity of TiO_2 with the inherent amphi-repellency of an amphiphobic material (Table 1), thus producing a material with enhanced self-cleaning properties. The amount of the TiO_2 NPs used for the production of the nanocomposite coating is carefully selected. This is extremely important for three reasons. First, as the coating is designed for the protection of glass, transparency should be maintained. Since the NPs are whitish, using a large amount of them will obscure transparency. Second, if a large amount of TiO_2 NPs is added into the fluorinated material, a textured surface will be produced which will suffer from poor mechanical durability as it was discussed previously. Finally, if the morphology of the coating changes largely, then the wetting properties and the desired amphiphobic character of the coating will be affected [57,58]. Prior to the study of the composite (fluorosilane +TiO_2) coatings, fluorosilane (without TiO_2) coatings are deposited on glass following the dip coating method. The effect of coating cycles on the transparency and wetting properties of treated glass are studied.

2. Experimental

2.1. Materials

Tridecafluorooctyltriethoxysilane (1H,1H,2H,2H-Perfluorooctyltriethoxysilane, PFOES) was purchased from Evonik (Dynasylan F8261) and titanium oxide (TiO_2) nanoparticles (NPs) with a diameter of 32nm were obtained from Alfa Aesar. Drops of various liquids were studied: distilled water, isopropanol (Sisco research Laboratories), diiodomethane (Acros Organics), N,N-dimethylformamide (DMF), and n-hexane (Sigma Aldrich). Metlhylene blue was obtained from Merck whereas aqueous hydrochloric acid solution (HCl) and sodium hydroxide (NaOH) were purchased from Penta Chemicals.

2.2. Coating preparation

The as received PFOES product was diluted in isopropanol (IPA), water and 5% HCl solution (83:10:5, w/w/w) to prepare a solution of 2 % w/w. The solution was stirred for 5h to hydrolyse the ethoxy groups resulting in reactive ethanol groups which can bond with the glass substrate.

Coatings were prepared according to the dip coating method. Clean microscope glass slides were immersed into the silane solution for 1 min, then withdrew and left to cure in ambient conditions for one day. Coatings which were deposited onto glass slides after immersing them into the PFOES solution only once are named hereafter as 1C. Coatings which were prepared after 2, 10 and 20 immersions, are named 2C, 10C and 20C, respectively.

TiO_2 NPs were dispersed into the silane solution. Dispersions with NP concentrations of 0.25, 0.5, 1.0 and 2.0% w/v were prepared. Glass slides were immersed into the dispersions twice resulting in coatings which are named as 2C+0.25Ti, 2C+0.5Ti, 2C+1Ti and 2C+2Ti.

2.3. Characterisation

Contact angles (CA) of drops (8 μL) of various liquids and contact angle hystereses (CAH) were measured using the ImageJ software. At least three drops were placed on different areas of coated

glass samples and average values were calculated. Scanning electron microscopy (SEM, TM3000, Hitachi) coupled with Energy Dispersive Spectroscopy (EDS, INCA x-act, Oxford instruments) was employed to study the surface structures of the coated glass.

The optical transparency of coated glass was assessed indirectly using colourimetry and directly using a spectrophotometer. In particular, for the colourimetric measurements, samples were placed onto a white reference surface. A PCE-CSM 1 spectrophotometer (PCE instruments,) was employed and the results were evaluated using the L^*, a^*, b^* coordinates of the CIE 1976 scale. The optical transmittance was measured using a UV–Vis spectrophotometer (V-750, Jasco).

The physical self-cleaning property of the 2C+0.25Ti coating was realized using IPA drops which removed methylene blue particles, used to contaminate the coated glass surface. A chamber equipped with a 300-W Osram Ultra Vitalux light (UV-A component) was used to study the photocatalytic decolourisation of methylene blue which was applied onto 2C+0.25Ti and 2C+2Ti coatings (chemical self-cleaning). Five drops (2 mL) of an aqueous solution of methylene blue (0.1% w/w) were placed on different areas of the samples which were then exposed to the UV light for a total period of 12h. For comparison, the procedure was applied on glass treated by the 2C coating and on uncoated glass. The same chamber was used to study the effect of the UV light on the wetting properties of the 2C and 2C+0.25Ti coatings.

For the abrasion resistance test, sandpaper (S/C W/P T9) under 200 g of loading was placed on top of coated glass. The sandpaper with the weight on top of it moved back and forth, in a reciprocating motion. This round-trip movement corresponded to a distance of 10 cm and was recorded as one cycle of abrasion. The 2C+0.25Ti and the 2C (control) coatings were subjected to this test.

Chemical resistance was checked with two tests. Drops of solutions, which were prepared using HCl or NaOH and corresponded to a pH range from 0 to 14, were placed on 2C+0.25Ti and 2C coatings and CAs were measured. Glass slides with 2C+0.25Ti and 2C coatings were immersed in aqueous and acetone baths at room temperature and left for 18 h. The wetting properties of the treated samples were tested through CA and CAH measurements of water and IPA drops.

The resistance of the 2C+0.25Ti coating against stains was investigated, according to two quick experiments. A long-lasting, smudge-proof and wear-resistant edding 300 marker was used to write on uncoated glass and glass coated by 2C+0.25Ti. Samples were allowed to dry for 5h and then they were wiped gently using a tissue paper. Moreover, glass coated by 2C+0.25Ti was immersed into a mud bath for more than 100 times. For comparison, uncoated glass was immersed into mud only once.

3. Results and discussion

The method to produce transparent composite coatings of PFOES and TiO_2 NPs that combine physical and chemical self-cleaning is implemented as follows. First, following the dip coating method, microscope glass slides are coated only by PFOES (without TiO_2 NPs) to study the effect of coating cycles on the transparency and wetting properties of the produced coatings (section 3.1). The goal is to select the optimum number of cycles which results in coatings with (i) low impact on glass transparency and (ii) enhanced physical self-cleaning properties i.e. enhanced amphi-repellent properties. In section 3.2, TiO_2 NPs are added to the coating formulation to induce chemical self-cleaning. Attention focuses on the selection of the appropriate NP concentration. This is crucial, because the selected NP concentration should be low enough to maintain glass transparency and the amphiphobic, amphi-repellent character of the coating (i.e. the physical self-cleaning property must be preserved) and high enough to induce chemical self-cleaning. Finally, in section 3.3 the durability and stain resistance of the selected coating are shown.

3.1. Effect of coating cycles on glass transparency and wetting properties

The effect of coating cycles on the transparency of treated glass is elucidated in Figure 1. For the colourimetric measurements (Figure 1a) the 1C, 2C, 10C and 20C coated samples were placed on white paper background and the colour changes (ΔE^*) induced by the coating applications were calculated as follows [59]:

$$\Delta E^* = \sqrt{(L_c^* - L_u^*)^2 + (a_c^* - a_u^*)^2 + (b_c^* - b_u^*)^2} \qquad (1)$$

where L^*, a^* and b^* are the brightness, the red–green component, and the yellow–blue component of the CIE 1976 scale, respectively. The "c" and "u" subscript characters indicate the coated and uncoated glass slides, respectively. The results of Figure 1a show that ΔE^* increases with the number of coating cycles. The coating thickness increases with the coating cycles and therefore the visual effect on glass substrate becomes more evident [60]. However, since for the 1C, 2C and 10C coated samples $\Delta E^*<3$ the appearance of glass is affected only insignificantly and the visual effect of the coatings cannot be easily perceived by human eye [61]. For the 20C coated sample ΔE^* is marginally larger than 3. The results obtained by colourimetry (Figure 1a) are confirmed by transmittance measurements of visible light which are shown in Figure 1b. Transmittance decreases progressively with the coating cycles. For the 1C and 2C coated samples transmittance remains >97% throughout the whole range of the visible spectrum (350-800 nm) whereas for the 10C and 20C coated samples it was >95% and >94%, respectively. Overall, the deposited coatings had only minor effects on the transmittance of visible light and this is confirmed in the photographs of Figure 1c.

Figure 2 shows the wetting properties of the 1C, 2C, 10C and 20C coatings. The variations of the contact angle (CA) and the contact angle hysteresis (CAH) of water and isopropanol (IPA) drops with the number of coating cycles are shown in Figures 2a and 2b, respectively. The corresponding graphs for the advancing and receding contact angles are provided in Figure S1 of the Supplementary material. The CAs of both liquids increase with the number of coating cycles (Figure 2a). According to the results of Figure 2b, a rapid decrease of the CAHs of both liquids is initially recorded: the CAs of water and IPA drops are roughly 16° and 23° for the 1C coating and become 8° and 9° respectively after two coating cycles i.e. for the 2C coating. Further increase of the number of coating cycles to 10 and 20, corresponding to the 10C and 20C coated samples, results in an increase of the CAHs of

both liquids. The origin of the variations of CA and CAH with respect to the coating cycles is revealed in the SEM-EDS mappings and SEM images of Figure 3.

Figures 3a and 3b show the distribution of fluorine (F) on the surfaces of the 1C and 2C coated samples. In the 1C surface, the coverage of the glass substrate by PFOES appears to be discontinuous, compared to the denser presence of F on the 2C surface. The non-uniform, discontinuous coverage of glass by PFOES with the application of one coating cycle can explain the elevated CAH which was reported in Figure 2b for the 1C surface. Better glass coverage was obtained by two coating cycles (2C surface, Figure 3b) leading to a major decrease of CAH (Figure 2b). The morphologies of the 1C, 2C, 10C and 20C surfaces are revealed in the SEM images of Figures 3c-3f. The image of Figure 3c shows that some scattered protrusions are formed on the 1C surface. These surface anomalies are formed during the curing and drying process of PFOES. They correspond to accumulated masses of the coating material, which can originate by a dewetting or shrinkage process of PFOES during drying [62]. The surface becomes smoother with the application of two coating cycles (surface 2C) which provide enough quantity of PFOES to cover the whole substrate surface (Figure 3d). However, some protrusions of small sizes can be observed on the 2C surface (Figure 3d). It has been reported that surface anomalies can emerge on a coating surface when a second coat is applied on an already-coated substrate [63]. The protrusions become larger and more frequent as the coating cycles increase to 10 and 20 (Figures 3e and 3f) [63]. This type of protrusions can act as obstacles for the motion of any liquid drop and this effect should be reflected to elevated CAHs [64]. According to the results of Figure 2b, the effect of the formed protrusions on CAH becomes noticeable for the 10C and 20C surfaces (elevated CAHs are reported in Figure 2b) in which both the size and the number of protrusions increase, compared to the 2C surface (Figures 3d-3f).

Based on the results reported in Figures 1 and 2, regarding the effects of coating cycles on the transparency and the amphi-repellent character of the resulting PFOES coating, the 2C coating is selected for further investigations. The 2C coated sample, gave the lowest WCA (Figure 3) and had a negligible effect on the transparency of glass (Figure 1).

3.2. Selection of the TiO_2 NP concentration

Two dip coating cycles were applied to treat glass samples using PFOES and TiO_2 NPs. The effect of the NP concentration on the optical transparency of coated glass was studied using colourimetry (Figure 4a) and spectrophotometry (Figure 4b). Figure 4a shows that the very low concentration of 0.25% w/w for TiO_2 NPs (2C+0.25Ti) had a small effect on the visual appearance of glass, as $\Delta E^*<3$. The transmittance of visible light on this coated sample (2C+0.25Ti) ranged from 98% to 93% (Figure 4b). Using higher NP concentrations for the preparation of the coatings has an important effect on optical transparency. In particular, according to the results of Figures 4a and 4b, the 2C+0.5Ti, 2C+1Ti and 2C+2Ti coatings induced a considerable effect on the appearance of glass ($\Delta E^*>3$) and affected the transmittance of visible light (350-800 nm) largely. The photographs of Figure 4c, reveal the progressive effect of the TiO_2 NP concentration on the optical transparency of glass. Overall, the results of Figure 4 suggest that only the 2C+0.25Ti coating can be considered for further investigations, as the optical transparency of glass is obscured when treated with NP concentration >0.25% w/w.

The wetting properties of the 2C+0.25Ti coating are revealed in the plots of Figure 5. For comparison the 2C (control) coated sample is included. Figures 5a and 5b show CAs of drops of water+IPA mixtures and drops of various liquids, respectively. CAs of drops of pure water and pure IPA are included in Figure 5a. The corresponding measurements for CAH are included in Figures 5c and 5d. Contact angles are plotted vs the surface tensions of the liquids which were obtained from the literature and are provided in Table S1 in the Supplementary material [65,66]. The results of Figures 5a and 5b show that CA increases with the liquid surface tension, on either 2C+0.25Ti or 2C surface. This tendency was previously reported for the wettabilities of other amphiphobic coatings, such as a composite of a fluorinated polyurethane and fluorodecyl polyhedral oligomeric silsesquioxane [52] and perfluoropolyether chains grafted on glass [56]. Moreover, the results of Figures 5a and 5b show

that the addition of TiO_2 NPs did not have any effect on CA, as practically the same CAs were measured on the two, 2C+0.25Ti and 2C, surfaces.

The CAHs of drops of water+IPA mixtures are low and practically constant and independent of the surface tension of the liquid (Figure 5c). Moreover, no statistically significant difference between the 2C+0.25Ti and 2C surfaces is reported, except for water drops. A difference of roughly 5.5° is measured in the water hysteresis between the two surfaces, with the 2C surface showing higher repellency i.e. lower hysteresis. Consequently, the results of Figure 5c reveal the repellent character of the 2C+0.25Ti surface which is almost comparable with that reported for the reference 2C coating. The repellent characters of both coatings are confirmed by the data of Figure 5d. Low (<15°) CAHs were measured on the 2C+0.25Ti surface for any of the tested liquids include in Figure 5d. A slightly higher CAH was measured for hexane drops on 2C.

The high-magnification SEM images included in Figure 5a show that the structures of the two surfaces (2C and 2C+0.25Ti) exhibit a slight difference. In particular, the 2C+0.25Ti surface is rougher compared to 2C. A higher density of small protrusions is observed on the 2C+0.25Ti surface than on 2C. That is because of the effect of the TiO_2 NPs which were added to the composite coating. It has been shown that adding NPs to siloxane coatings leads to the formation of protrusions which increase surface roughness [37,58,59]. However, based on the CA and CAH measurements it can be concluded that the small difference in the surface structures of the two coatings is not capable to induce a noticeable difference in their wetting properties.

The advancing (ADV) and receding (REC) contact angles which were used to calculate the hystereses in Figure 5 are given in Figure S2 of the Supplementary material. Using these ADV and REC angles the force per unit length (F) which is needed to start a drop moving over a solid surface can be calculated as follows [67]:

$$F = \gamma_L(\cos REC - \cos ADV) \quad (2)$$

The calculated F is given in Figure S3 of the Supplementary material for drops of water+IPA mixtures and drops of various liquids. It is seen that almost the same critical force F is needed to start a drop moving on either the 2C or the 2C+0.25Ti surface (Figure S3). A noteworthy difference is observed only for the water drops, as the 2C+0.25Ti appears to be slightly more adhesive, than the 2C surface, corresponding to a slightly higher F. In sum, Figure S3 offers support to the message delivered by Figure 5: the amphi-repellent character of the 2C+0.25Ti surface is comparable with that of the 2C surface; a small difference between the two surfaces is observed only on water repellency.

Judging from the overall results of Figure 5 it is stated that the addition of the small amount (0.25% w/w) of TiO_2 in the coating's recipe did not have any major effect on the wetting properties of the coating. The extreme repellencies originate from the low surface energy of PFOES which can be calculated using the OWRK (Owens-Wendt-Rabel-Kaelble) method [68]:

$$\gamma_L(1 + \cos CA) = 2\left[\sqrt{\gamma_L^d \gamma_S^d} + \sqrt{\gamma_L^p \gamma_S^p}\right] \quad (3)$$

$$\gamma_S = \gamma_S^d + \gamma_S^p \quad (4)$$

where γ_L^d and γ_L^p are the dispersive and polar components of the surface free energy of the liquid (γ_L); γ_S^d and γ_S^p are the corresponding components of the surface free surface of the solid (γ_S). Using values of γ_L^d and γ_L^p for water and diiodomethane, which are included in Table S2 [68] of the Supplementary material and CA values for the 2C surface, the surface free energy of PFOES was calculated and found 10.58 mJ/m^2. It should be stressed that the application of the OWRK method includes the assumption that the solid surface is perfectly smooth [69], a condition that is not always taken into careful consideration. The SEM image of Figure 3b revealed that the 2C surface is not perfectly smooth and therefore the reported low value of γ_S (=10.58 mJ/m^2) can be considered as an approximation.

In Figure 6 some important properties of the 2C+0.25Ti coating are demonstrated. In particular, Figure 6a shows static drops of various liquids, including water, IPA, DMF, diiodomethane, salad (olive) oil, coffee with milk and water-based ink, on the 2C+0.25Ti surface. Sliding drops of water and IPA on tilted coated glass are shown in Figure 6b, revealing the repellent character of the 2C+0.25Ti surface. The repellent character of the coating is further demonstrated in Figure 6c in comparison with uncoated glass. A water drop, dyed with methylene blue, slides off the coated glass while it leaves a blue trace on uncoated glass. The transparency of the 2C+0.25Ti surface is demonstrated in the photographs of Figure 6d. Finally, the self-cleaning scenario is shown in the successive snapshots of Figure 6e. Glass coated by 2C+0.25Ti was contaminated with particles of methylene blue which were removed by IPA drops. The use of IPA, instead of water drops which are most commonly used to realise the self-cleaning effect, stresses the amphiphobic character of the 2C+0.25Ti surface.

The transparency and the physical self-cleaning property of the 2C+0.25Ti coated sample, originated by the amphi-repellent character of the deposited coating, were discussed and revealed in Figures 4-6. However, the ability of TiO_2 to induce chemical self-cleaning, when it is used in such very small amount (0.25% w/w), is questioned. For this reason, glass coated by 2C+0.25Ti was contaminated with methylene blue and the removal of the dye under the effect of the UV radiation was measured. For comparison, three more samples were included in the study. Uncoated glass and 2C coated sample were treated with the same procedure to report the removal of the dye due to the UV radiation and without the involvement of the photocatalytic mechanism. Moreover, a sample with a high content in TiO_2 NPs (i.e. 2C+2Ti coating) was included, as this is expected to induce sufficient chemical self-cleaning due to photocatalysis. The results are analysed with respect to the relative cleaning efficacy (CE%) which was calculated using the following formula [70,71]:

$$CE\% = \left(\frac{\Delta E^*_{stained} - \Delta E^*_{UV}}{\Delta E^*_{stained}}\right)100 \qquad (5)$$

where $\Delta E^*_{stained}$ is the colour change after the deposition of methylene blue and before the UV treatment and ΔE^*_{UV} is the colour change recorded on the same sample after the UV treatment. Both colour changes are measured with respect to the original, unstained samples. Therefore, in the ideal case of the total removal of the stain ΔE^*_{UV} becomes 0 and therefore $CE\% = 100$. The results for the four investigated samples are shown in Figure 7. The removal of the dye from uncoated glass was imperceptible, as it corresponds to a very small CE%. A large degree of degradation of methylene blue was achieved on the 2C coated sample, suggesting that the repellent character of PFOES is capable to largely promote the removal of the dye, compared to the uncoated glass. Dye removal was further promoted by the photocatalytic effect of TiO_2 resulting in even larger values of CE% for the 2C+0.25Ti coating. Although the contribution of TiO_2 on the removal of the dye is clear, it is interesting to note that the relative increase of the CE% between the 2C and 2C+0.25 coatings is much smaller compared to the dramatic increase of CE% between the 2C and the uncoated samples. However, this relative increase of the CE% between the 2C and 2C+0.25 coatings is comparable with the corresponding increase of CE% which was achieved when the concentration of TiO_2 was increased by a factor of 8, that is from 0.25% w/w (2C+0.25C coating) to 2% w/w (2C+2Ti coating). Therefore, the gain in chemical self-cleaning achieved by an increased TiO_2 concentration is extremely small compared to the forbidding penalty imposed on glass transparency. From the results of Figure 7, it is possible to conclude that sufficient chemical self-cleaning is induced by the 2C+0.25Ti coating which furthermore is transparent to visible light (Figure 4) and shows amphi-repellent wetting properties i.e. physical self-cleaning (Figures 5 and 6).

3.3. Durability and stain resistance

The mechanical durability of the 2C+0.25Ti coating was studied with the abrasion test and the results are shown in Figure 8. For comparison, the 2C coating is included. According to Figure 8a the CAs of either water or IPA drops remained practically unaffected after subjecting any of the two surfaces

in 100 cycles of harsh abrasion. Moreover, the results of Figure 8a suggest that adding TiO_2 NPs did not have any major effect on the mechanical durability of the coating, as the 2C and the 2C+0.25Ti surfaces gave comparable CAs. This result is absolutely clear for the CAs of water drops. For the IPA drops, at elevated abrasion cycles (≥40) slightly higher CAs can be noticed on the composite coating (2C-0.25Ti) than on the 2C surface. However, the differences of the IPA CAs on the two coatings are small after 40, 60 and 80 abrasion cycles and almost within the experimental error after 100 cycles. Abrasion tends to affect the repellent characters of both 2C-0.25Ti and 2C coatings, as the CAHs increase with abrasion cycles, as revealed in the results of Figure 8b. Roughly, the initial CAHs of either water or IPA drops varied around 10° and increased to around 20° after 100 cycles of harsh abrasion. Similar to what it what noticed for the CAs in Figure 8a, a slight difference on the wettabilities of the two coatings by IPA, after applying 40, 60 and 80 abrasion cycles, is supported by the CAH results of Figure 8b. However, this slight difference of the IPA CAHs which were measured on the two different coatings, vanishes after 100 abrasion cycles. The main message delivered from the results of Figure 8 is that the small amount of TiO_2 NPs which was added to the polymer matrix to induce chemical self-cleaning did not affect the durability of the coating, against abrasion. Overall, the mechanical stabilities of the coatings with (2C-0.25Ti) and without (2C) TiO_2 NPs were comparable.

The stability of the 2C-0.25Ti coating, in comparison with the reference 2C coating, against the UV radiation is revealed in Figure 9. The latter shows that the wetting properties of the composite (2C-0.25Ti) coating were overall not affected by the UV radiation. CAs and CAHs of both water and IPA drops on the 2C-0.25Ti coating were practically unaffected by the accelerating UV ageing treatment. Only a slight variation of the CAs of water drops, before and after exposing the 2C-0.25Ti surface in UV radiation, can be noticed in Figure 9a which, however, is almost within the experimental error. The reference, 2C coating was also quite stable against the UV radiation, although a slight increase of the CA of water drops (Figure 9b) can be noticed. Overall, the results of Figure 9 suggest that both, 2C+0.25Ti and 2C, coatings were equally stable against the effects of the UV radiation.

CAs of drops, which corresponded to a wide range of pH, are included in Figure 10a. It is seen that CAs on both 2C+0.25Ti and 2C remain stable and are not affected by the drop pH. Furthermore, 2C+0.25Ti and 2C coated samples were immersed in aqueous and acetone drops for 18 h. Samples were removed from the baths and CAs and CAHs of both water and IPA drops were measured. The results are included in Figures 10b-10d and show that neither of the two baths had an effect on the amphiphobic and repellent characters of the 2C+0.25Ti and the 2C (control) coatings.

Two experiments were performed to test the stain resistance and anti-smudge performance of the 2C+0.25Ti coating. The photographs of Figure 11a show that a wear-resistant editing marker writes well on uncoated glass leaving continue lines, whereas it leaves only discontinuous small marks on glass which was coated by 2C+0.25Ti. The small marks on coated glass are wiped away easily using paper tissue (Figure 11b). On the contrary, the continues lines on the uncoated glass remained unchanged after wiping (Figure 11b). The photographs of Figure 11c show that mud does not stick on glass coated by the 2C+0.25Ti composite. Three consecutive snapshots are shown in Figure 11c to illustrate the experiment. Coated glass was dipped into mud, left for around 2 s and then it was taken out. Because of the repellent character of the 2C+0.25Ti coating the sample remained clean. The process repeated for more than 100 times and the coated surface was not contaminated. On the contrary, mud stuck on the surface of uncoated glass which became soiled even after one dip cycle (Figure 11d). In sum, the 2C+0.25Ti coating has very good stain resistance and anti-smudge performance, comparable to those reported for smooth, low surface energy, amphiphobic repellent coatings [48,53,56]. In contrast to the 2C+0.25Ti surface, these previously investigated coatings did not have the ability of chemical self-cleaning as photocatalytic agents were not included in their production recipes [48,53,56].

4. Conclusions

The production of a transparent and robust coating on glass which combines physical self-cleaning and stain resistance, through its amphiphobic and amphi-repellent character, with chemical self-cleaning, through photocatalytic activity, is reported. The coating consists of PFOES (1H,1H,2H,2H-

Perfluorooctyltriethoxysilane) and TiO_2 NPs. First, only PFOES was applied on glass following the dip coating method without using TiO_2 NPs. It was shown that optical transparency of treated glass and transmittance of visible light decrease progressively with the coating cycles (Figure 1). The latter affect also the morphology (Figure 3) and therefore the wetting properties (Figure 2) of the deposited coating. Using a concentration of 2% w/w for PFOES it was shown that the application of two coating cycles (2C) results in maximum repellency and preserves the optical transparency of treated glass. TiO_2 NPs were then added into the selected 2C coating in various concentrations. It was shown that optical transparency of treated glass and transmittance of visible light decrease with the NP concentration (Figure 4). Consequently, a very low concentration (0.25% w/w) of TiO_2 NPs was selected for further studies, as optical transparency (Figure 4) and amphi-repellent properties (Figures 5 and 6) were preserved by the -so called- 2C+0.25Ti coatings. The 2C+0.25Ti coating showed sufficient chemical self-cleaning induced by the photocatalytic activity of TiO_2 (Figure 7). The coating showed very good mechanical stability against abrasion (Figure 8), resistance to degradation effects induced by the UV radiation (Figure 9), chemical stability (Figure 10) and stain resistance and anti-smudge performance (Figure 11).

Acknowledgements

The authors would like to thank associate professor Theodoros Lazarides (Aristotle University of Thessaloniki) for his assistance with spectrophotometry and the transmittance measurements. The financial support of Abu Dhabi University through the Internal Research, Innovation and Impact Grant No. 19300626 to Ioannis Zuburtikudis is greatly acknowledged.

References

1. T. Minaai, K.D. Sanderson, Self-cleaning glass, in: A. Fujishima, H. Irie, X. Zhang, D.A. Tryk (Eds.), Handbook of Self-Cleaning Surfaces and Materials: From Fundamentals to Applications, Wiley-VCH GmbH, Weinheim, 2023, pp. 449–459.

2. B. Sedighian, R. Jafari, M. Mahdavian, M. Nasiri, Using colorimetric methods to analyze the impact of acrylic binders' physical-chemical factors on dirt-pickup resistance of white façade coatings, Prog. Org. Coat. 166 (2022) 106804.
3. Y.N. Chanchangi, A. Ghosh, S. Sundaram, T.K. Mallick, Dust and PV performance in Nigeria: a review, Renew. Sustain. Energy Rev. 121 (2020) 109704.
4. T.Y. Tanaka, C. Chiba, A numerical study of the contributions of dust source regions to the global dust budget, Glob Planet Chang 52 (2006) 88–104.
5. S. Engelstaedter, I. Tegen, R. Washington, North African dust emissions and transport, Earth-Sci. Rev. 79 (2006) 73–100.
6. N.J. Middleton, Desert dust hazards: A global review, Aeolian Res. 24 (2017) 53–63.
7. E. Svinterikos, I. Zuburtikudis, H.A. Khalifeh, S.F.A. Ali, Multifunctional polymer-based coatings for outdoor glass surfaces: A state of the art, Advanced Industrial and Engineering Polymer Research 6 (2023) 310–332.
8. Z. Liu, P. Tu, Y. Ji, Z. Cai, H. Wu, B. Xu, An eco-friendly and durable anti-fogging coating based on sulfobetaines and silicones, Prog. Org. Coat. 177 (2023) 107413.
9. L. Chen, J. Wang, J. Ye, L. Wang, Z. Liu, S. Zhuo, X. Ouyang, X. Zhou, Y. Wang, W. Chen, Y. Liu, One-step assembly of organic-inorganic hybrid coatings with superior thermal insulation, sustainable antifogging and self-cleaning capabilities, Prog. Org. Coat. 184 (2023) 107878.
10. C. Feng, T. Gou, J. Li, Y. Cai, P. He, J. Huang, Y. Wen,Y. Ma, Z. Zhang A highly transparent polymer coating on the glass with broadband antireflection, antifogging and antifouling properties, Mater. Res. Express 6 (2019) 075319.
11. A. Fujishima, K. Honda, Electrochemical photolysis of water at a semiconductor electrode, Nature 238 (1972) 37–38.

12. R. Wang, K. Hashimoto, A. Fujishima, M. Chikuni, E. Kojima, A. Kitamura, M. Shimohigoshi, T. Watanabe, Light-induced amphiphilic surfaces, Nature 388 (1997) 431–432.
13. K. Nakata, A. Fujishima, TiO_2 photocatalysis: design and applications. J. Photoch. Photobio. C. 13 (2012) 169–189.
14. V.A. Maiorov, Self-cleaning glass, Glass Phys. Chem. 45 (2019) 161–174.
15. Y. Zhang, S. Zhang, S. Wu, Room-temperature fabrication of TiO_2-PHEA nanocomposite coating with high transmittance and durable superhydrophilicity, Chem. Eng. J. 371 (2019) 609–617.
16. M.M. Mutter, S.G. Khalil, M.E. Ismael, R.H. Jabbar, Preparation of TiO_2:PMMA:PVA nanocomposite thin film as a smart coating as the self-cleaning application, J. Phys. Conf. Ser. 2322 (2022) 012072.
17. A.J. Gayle, J.D. Lenef, P.A. Huff, J. Wang, F. Fu, G. Dadheech, N.P. Dasgupta, Visible-light-driven photocatalysts for self-cleaning transparent surfaces, Langmuir 38 (2022) 11641−11649.
18. A.A. Ismail, L. Al-Hajji, I.S. Azad, A. Al-Yaqoot, N. Habibi, M. Alseidi, S. Ahmed, Self-cleaning application of mesoporous ZnO, TiO_2 and Fe_2O_3 films with the accommodation of silver nanoparticles for antibacterial activity, J. Taiwan Inst. Chem. E. 142 (2023) 104627.
19. W. Barthlott, C. Neinhuis, Purity of the sacred lotus, or escape from contamination in biological surfaces, Planta 202 (1997) 1–8.
20. F. Cirisano, M. Ferrari, Superhydrophobicity and durability in recyclable polymers coating, Sustainability 13 (2021) 8244.
21. X. Liu, C. Gao, C. Fu, Y. Xi, P. Fatehi, J.R. Zhao, S. Wang, M.E. Gibril, F. Kong, Preparation and performance of lignin-based multifunctional superhydrophobic coating, Molecules 27 (2022) 1440.

22. X. Huang, M. Sun, X. Shi, J. Shao, M. Jin, W. Liu, R. Zhang, S. Huang, Y. Ye, Chemical vapor deposition of transparent superhydrophobic anti-Icing coatings with tailored polymer nanoarray architecture, Chem. Eng. J. 454 (2023) 139981.

23. J. Wang, K. Li, J. Zhang, J. Feng, Transparent and superhydrophobic FHA/SiO_2 coatings with obvious anti-soiling performance for photovoltaic modules, Prog. Org. Coat. 183 (2023) 107679.

24. R.S. Sutar, S. Nagappan, A.K. Bhosale, K.K. Sadasivuni, K.-H. Park, C.-S. Ha, S.S. Latthe, Superhydrophobic Al_2O_3-polymer composite coating for self-cleaning applications, Coatings 11 (2021) 1162.

25. Y. Liu, R. Sun, B. Jin, T. Li, L. Yao, L. Feng, J. He, Superhydrophobic VO_2 nanoparticle/PDMS composite films as thermochromic, anti-icing, and self-cleaning coatings, ACS Appl. Nano Mater. 5 (2022) 5599-5608.

26. C. Peng, Z. Chen, M.K. Tiwari, All-organic superhydrophobic coatings with mechanochemical robustness and liquid impalement resistance, Nat. Mater. 17 (2018) 355-360.

27. P. Wang, C. Li, D. Zhang, Recent advances in chemical durability and mechanical stability of superhydrophobic materials: Multi-strategy design and strengthening, J. Mater. Sci. Technol. 129 (2022) 40–69.

28. K. Wang, S. Yu, W. Li, Y. Song, P. Gong, M. Zhang, H. Li, D. Sun, X. Yang, X. Wang, Superhydrophobic and photocatalytic synergistic Self-Cleaning ZnS coating, Appl. Surf. Sci. 595 (2022) 153565.

29. C. Urata, B. Masheder, D.F. Cheng, A. Hozumi, Unusual dynamic dewetting behavior of smooth perfluorinated hybrid films: Potential advantages over conventional textured and liquid-infused perfluorinated surfaces, Langmuir 29 (2013) 12472-12482.

30. A.B.D. Cassie, S. Baxter, Wettability of porous surfaces, Trans. Faraday Soc. 40 (1944) 546–951

31. R.N. Wenzel, Resistance of solid surfaces to wetting by water, Eng. Chem. 28 (1936) 988–994.

32. M. Sbragaglia, A.M. Peters, C. Pirat, B.M. Borkent, R.G.H. Lammertink, M. Wessling, D. Lohse, Spontaneous breakdown of superhydrophobicity, Phys. Rev. Lett. 99 (2007) 156001.

33. D. Murakami, H. Jinnai, A. Takahara, Wetting transition from the Cassie−Baxter state to the Wenzel state on textured polymer surfaces, Langmuir 30 (2014) 2061−2067.

34. K. Liu, Y. Tian, L. Jiang, Bio-inspired superoleophobic and smart materials: Design, fabrication, and application, Prog. Mater. Sci. 58 (2013) 503–564.

35. A. Susarrey-Arce, A.G. Marín, H. Nair, L. Lefferts, J. G. E. Gardeniers, D. Lohse, A. van Houselt, Absence of an evaporation-driven wetting transition on omniphobic surfaces, Soft Matter, 2012, 8, 9765.

36. H. Zhu, S. Cai, G. Liao, Z.F. Gao, X. Min, Y. Huang, S. Jin, F. Xia, Recent advances in photocatalysis based on bioinspired superwettabilities, ACS Catal. 11 (2021) 14751−14771.

37. I. Karapanagiotis, P.N. Manoudis, Superhydrophobic and superamphiphobic materials for the conservation of natural stone: An overview, Constr. Build. Mater. 320 (2022) 126175.

38. T. Kamegawa, Y. Shimizu, H. Yamashita, Superhydrophobic surfaces with photocatalytic self-cleaning properties by nanocomposite coating of TiO_2, and polytetrafluoroethylene, Adv. Mater. 24 (2012) 3697–3700.

39. X. Zhang, S. Liu, A. Salim, S. Seeger, Hierarchical structured multifunctional self-cleaning material with durable superhydrophobicity and photocatalytic functionalities, Small 15 (2019) 1901822.

40. H. Zhu, L. Wu, X. Meng, Y. Wang, Y. Huang, M. Lin, F. Xia, An anti-UV superhydrophobic material with photocatalysis, self-cleaning, self-healing and oil/water separation functions, Nanoscale 12 (2020) 11455–11459.

41. J. Liu, L. Ye, Y. Sun, M. Hu, F. Chen, S. Wegner, V. Mailänder, W. Steffen, M. Kappl, H.-J. Butt, Elastic superhydrophobic and photocatalytic active films used as blood repellent dressing, Adv. Mater. 32 (2020) 1908008.

42. H. Zhu, Y. Huang, S. Zhang, S. Jin, X. Lou, F. Xia, A universal, multifunctional, high-practicability superhydrophobic paint for waterproofing grass houses, NPG Asia Mater. 13 (2021) 47.

43. T. Zhu, Y. Cheng, J. Huang, J. Xiong, M. Ge, J. Mao, Z. Liu, X. Dong, Z. Chen, Y. Lai, A transparent superhydrophobic coating with mechanochemical robustness for anti-icing, photocatalysis and self-cleaning, Chem. Eng. J. 399 (2020) 125746.

44. S. Sunny, N. Vogel, C. Howell, T. L. Vu, J. Aizenberg, Lubricant-infused nanoparticulate coatings assembled by layer-by-layer deposition, Adv. Funct. Mater. 24 (2014) 6658–6667.

45. M.J. Kratochvil, M. A. Welsh, U. Manna, B.J. Ortiz, H.E. Blackwell, D.M. Lynn, Slippery liquid-infused porous surfaces that prevent bacterial surface fouling and inhibit virulence phenotypes in surrounding planktonic cells, ACS Infect. Dis. 2 (2016) 509−517.

46. M. Zhang, Q. Liu, J. Liu, J. Yu, J. Wang, Self-healing liquid-infused surfaces with high transparency for optical devices, MRS Commun. 9 (2019) 92–98.

47. X. Tan, Y. Zhang, X. Liu, S. Xi, Z. Yan, Z. Liu, T. Shi, G. Liao, Employing micro pyramidal holes and porous nanostructures for enhancing the durability of lubricant-infused surfaces in anti-icing, Surf. Coat. Tech. 405 (2021) 126568.

48. F. Mayoussi, Y. Chen, D. Mössner, S.F. Corredor, A. Goralczyk, M. Mader, A. Warmbold, F. Kotz-Helmer, D. Helmer, B.E. Rapp, Smooth transparent omniphobic coatings with remarkable liquid repellence, Adv. Mater. Interfaces 9 (2022) 2201080.

49. G. Han, T.-B. Nguyen, S. Park, Y. Jung, J. Lee, H. Lim, Moth-eye mimicking solid slippery glass surface with icephobicity, transparency, and self-healing, ACS Nano 14 (2020) 10198−10209.

50. C. Urata, B. Masheder, D.F. Cheng, A. Hozumi, Unusual dynamic dewetting behavior of smooth perfluorinated hybrid films: Potential advantages over conventional textured and liquid-infused perfluorinated surfaces, Langmuir 29 (2013) 12472−12482.

51. J. Jiang, G. Zhang, Q. Wang, Q. Zhang, X. Zhan, F. Chen, Novel fluorinated polymers containing short perfluorobutyl side chains and their super wetting performance on diverse substrates, ACS Appl. Mater. Interfaces 8 (2016) 10513−10523.

52. M. Boban, K. Golovin, B. Tobelmann, O. Gupte, J.M. Mabry, A. Tuteja, Smooth, All-solid, low-hysteresis, omniphobic surfaces with enhanced mechanical durability, ACS Appl. Mater. Interfaces 10 (2018) 11406−11413.

53. P. Gao, Y. Wang, H. Wang, J. Wang, X. Men, Z. Zhang, Y. Lu, Liquid-like transparent and flexible coatings for anti-graffiti applications, Prog. Org. Coat. 161 (2021) 106476.

54. M. Psarski, G. Celichowski, E. Bystrzycka, D. Pawlak, J. Grobelny, M. Cichomski, Vapor phase deposition of fluoroalkyl trichlorosilanes on silicon and glass: Influence of deposition conditions and chain length on wettability and adhesion forces, Mater. Chem. Phys. 204 (2018) 305-314.

55. J. Liu, Y. Sun, X. Zhou, X. Li, M. Kappl, W. Steffen, H.-J. Butt, One-step synthesis of a durable and liquid-repellent poly(dimethylsiloxane) coating, Adv. Mater. 33 (2021) 2100237.

56. Z. Ma, Y. Wu, R. Xu, Z. Li, Y. Liu, J. Liu, M. Cai, W. Bu, F. Zhou, Robust hybrid omniphobic surface for stain resistance, ACS Appl. Mater. Interfaces 13 (2021) 14562−14568.

57. Q.F. Xu, Y. Liu, F.-J. Lin, B. Mondal, A.M. Lyons, Superhydrophobic TiO_2−polymer nanocomposite surface with UV induced reversible wettability and self-cleaning properties, ACS Appl. Mater. Interfaces 5 (2013) 8915−8924.

58. P.N. Manoudis, I. Karapanagiotis, A. Tsakalof, I. Zuburtikudis, C. Panayiotou, Superhydrophobic composite films produced on various substrates, Langmuir 24 (2008) 11225–11232.

59. P.N. Manoudis, I. Karapanagiotis, A. Tsakalof, I. Zuburtikudis, B. Kolinkeová, C. Panayiotou, Superhydrophobic films for the protection of outdoor cultural heritage assets, Appl. Phys. A - Mater. 97 (2009) 351–360.

60. P. Malliga, J. Pandiarajan, N. Prithivikumaran, K. Neyvasagam, Effect of film thickness on structural and optical properties of TiO_2 thin films, Proceedings of the "International Conference on Advanced Nanomaterials & Emerging Engineering Technologies" (ICANMEET-20J3), New Delhi, India, July 24-26, 2013, pp. 488–491.

61. J.D. Rodrigues, A. Grossi, Indicators and ratings for the compatibility assessment of conservation actions, J. Cult. Herit. 8 (2007) 32–43.

62. I. Karapanagiotis, D.F. Evans, W.W. Gerberich, Nucleation processes for dewetting initiation of thin polymer films, Langmuir 17 (2001) 3266–3272.

63. M. Shimokawa, H. Yoshida, T. Komatsu, R. Omachi, K. Kudo, Emergence of wrinkles during the curing of coatings, Gels 4 (2018) 41.

64. P.N. Manoudis, I. Karapanagiotis, A. Tsakalof, I. Zuburtikudis, C. Panayiotou, Superhydrophobic composite films produced on various substrates, Langmuir 24 (2008) 11225–11232.

65. G. Vásquez, E. Alvarez, J.M. Navaza, Surface tension of alcohol + water from 20 to 50 °C, J. Chem Eng Data 40 (1995) 611–614.

66. https://www.dataphysics-instruments.com/Downloads/Surface-Tensions-Energies.pdf. Accessed in Nov 27, 2023.

67. W. Chen, A.Y. Fadeev, M.C. Hsieh, D. Öner, J. Youngblood, T.J. McCarthy, Ultrahydrophobic and ultralyophobic surfaces: some comments and examples Langmuir 15 (1999) 3395–3399.

68. D.K. Owens, R.C. Wendt, Evaluation of the surface free energy of polymers, J. Appl. Polym. Sci. 13 (1969) 17411–1747.

69. W.S.Y. Wong, M.S. Kiseleva, S. Zhou, M. Junaid, L. Pitkänen, R.H.A. Ras, Design of fluoro-free surfaces super-repellent to low-surface-tension liquids, Adv. Mater. 35 (2023) 2300306.
70. M. Lettieri, M. Masieri, M. Frigione, Novel nano-filled coatings for the protection of built heritage stone surfaces, Nanomaterials 11 (2021) 301.
71. M. Lettieri, M. Masieri, M. Aquaro, D. Dilorenzo, M. Frigione, Eco-friendly protective coating to extend the life of art-works and structures made in porous stone materials, Coatings 11 (2021) 1270.

TABLE CAPTIONS

Table 1. Materials which have been used to coat glass surfaces and to induce self-cleaning properties.

FIGURE CAPTIONS

Figure 1. (a) Colour change (ΔE^*), (b) % transmittance and (c) photographs of glasses, treated by different dip coating cycles: from 1 (coated sample 1C) to 20 (coated sample 20C) cycles. Uncoated glass is included in (b) and (c).

Figure 2. (a) Contact angles (CA) and contact angle hysteresis (CAH) of water and isopropanol (IPA) drops vs the coating cycles which were applied to treat glass.

Figure 3. EDS maps of F on the surfaces of (a) 1C and (b) 2C coated samples and SEM images of the surfaces of (c) 1C, (d) 2C, (e) 10C and (f) 20C coated samples.

Figure 4. (a) Colour change (ΔE^*), (b) % transmittance and (c) photographs of glasses, treated by coatings which were prepared using two dip coating cycles (2C) and different TiO_2 NP concentrations: 0.25, 0.5, 1 and 2% w/w. The 2C coated sample (without TiO_2 NPs) is included in (a) and (b) and uncoated glass in (b) and (c).

Figure 5. CA of drops of (a) water+IPA mixtures and (b) various liquids, on 2C and 2C+0.25Ti coatings on glass. CAH of drops of (c) water+IPA mixtures and (d) various liquids, on 2C and 2C+0.25Ti coatings on glass. CA and CAH are plotted vs the surface tension of the liquid. The tested liquids in (b) and (c) are water, diiodomethane (methylene iodide MI), N,N-dimethylformamide (DMF), isopropanol (IPA) and n-hexane (Hex). SEM images showing the surface structures of the 2C and 2C+0.25Ti coatings are included in (a).

Figure 6. Various properties of glass coated by 2C+0.25Ti. (a) Static drops of various liquids on coated glass. (b) Sliding of water and IPA drops on tilted coated glass. (c) Water drops coloured with methylene blue hit coated (left) and uncoated (right) titled glass surface. (d) Transparency of the 2C+0.25Ti coating (left) in comparison with uncoated (right) glass. (e) The self-cleaning scenario is realised with drops of IPA on contaminated coated glass.

Figure 7. Cleaning efficacies (CE%) of coated (2C, 2C+0.25Ti and 2C+2Ti) and uncoated glass slides, which were contaminated with methylene blue, were calculated using equation 5 for various periods of treatment under the UV light.

Figure 8. Stability of the 2C-0.25Ti coating in comparison with the 2C coating, against abrasion. (a) CA and (b) CAH of water and IPA drops vs the number of abrasion cycles.

Figure 9. Stability of the 2C-0.25Ti coating in comparison with the 2C coating, against accelerating ageing conditions (UV radiation). CA of (a) water and (b) IPA drops before and after ageing. CAH of (c) water and (d) IPA drops before and after ageing.

Figure 10. Chemical stability of the 2C-0.25Ti coating in comparison with the 2C coating. CA of (a) drops of aqueous solutions vs the drop pH. CA of (b) water and (c) IPA drops before and after immersing the coatings in aqueous and acetone baths. CAH of (b) water and (c) IPA drops before and after immersing the coatings in aqueous and acetone baths.

Figure 11. (a) An editing marker leaves a continue lines on uncoated glass and retracts into small droplets on glass coated by 2C+0.25Ti. (b) Wiping did not have any effect on written uncoated glass but removed the small droplets from the 2C+0.25Ti surface. (c) Glass coated by 2C+0.25Ti was kept

clean, after immersing it into a mud bath for more than 100 times. (d) Uncoated glass picks up mud after the first immersion.

SUPPLEMENTARY MATERIAL

Robust and transparent smooth amphi-repellent coating with physical and chemical self-cleaning properties

Panagiotis N. Manoudis[1], Ioannis Zuburtikudis[2], Hadil Abu Khalifeh[2] and Ioannis Karapanagiotis[3*]

[1]Lysis Consulting P.C., 55534 Thessaloniki, Greece
[2]Department of Chemical Engineering, Abu Dhabi University (ADU), P.O. Box 59911, Abu Dhabi, United Arab Emirates
[3]Department of Chemistry, Aristotle University of Thessaloniki, 54124 Thessaloniki, Greece

*karapana@chem.auth.gr

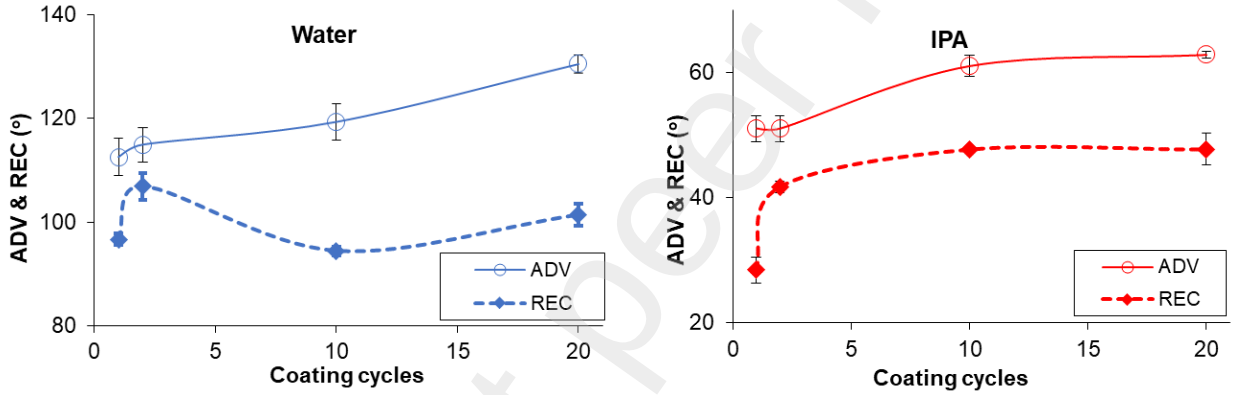

(a) (b)

Figure S1. Advancing (ADV) and receding (REC) contact angles of (a) water and (b) isopropanol drops vs the coating cycles which were applied to treat glass.

Table S1. Surface tensions of liquids used in the study. The values were obtained from literature as indicated.

Liquid	Surf tension (mN/m)	Liquid	Surf tension (mN/m)
Water[(a)]	72.75	Water[(a)]	72.75
5% IPA[(a)]	50.32	Diiodomethane[(b)]	50.80
20% IPA[(a)]	31.16	DMF[(b)]	37.10
50% IPA[(a)]	24.78	IPA[(a)]	21.74
IPA[(a)]	21.74	n-hexane[(b)]	18.43

[(a)]G. Vásquez, E. Alvarez, J.M. Navaza, Surface tension of alcohol + water from 20 to 50 °C, J. Chem Eng Data 40 (1995) 611–614.
[(b)]https://www.dataphysics-instruments.com/Downloads/Surface-Tensions-Energies.pdf. Accessed in Nov 27, 2023.

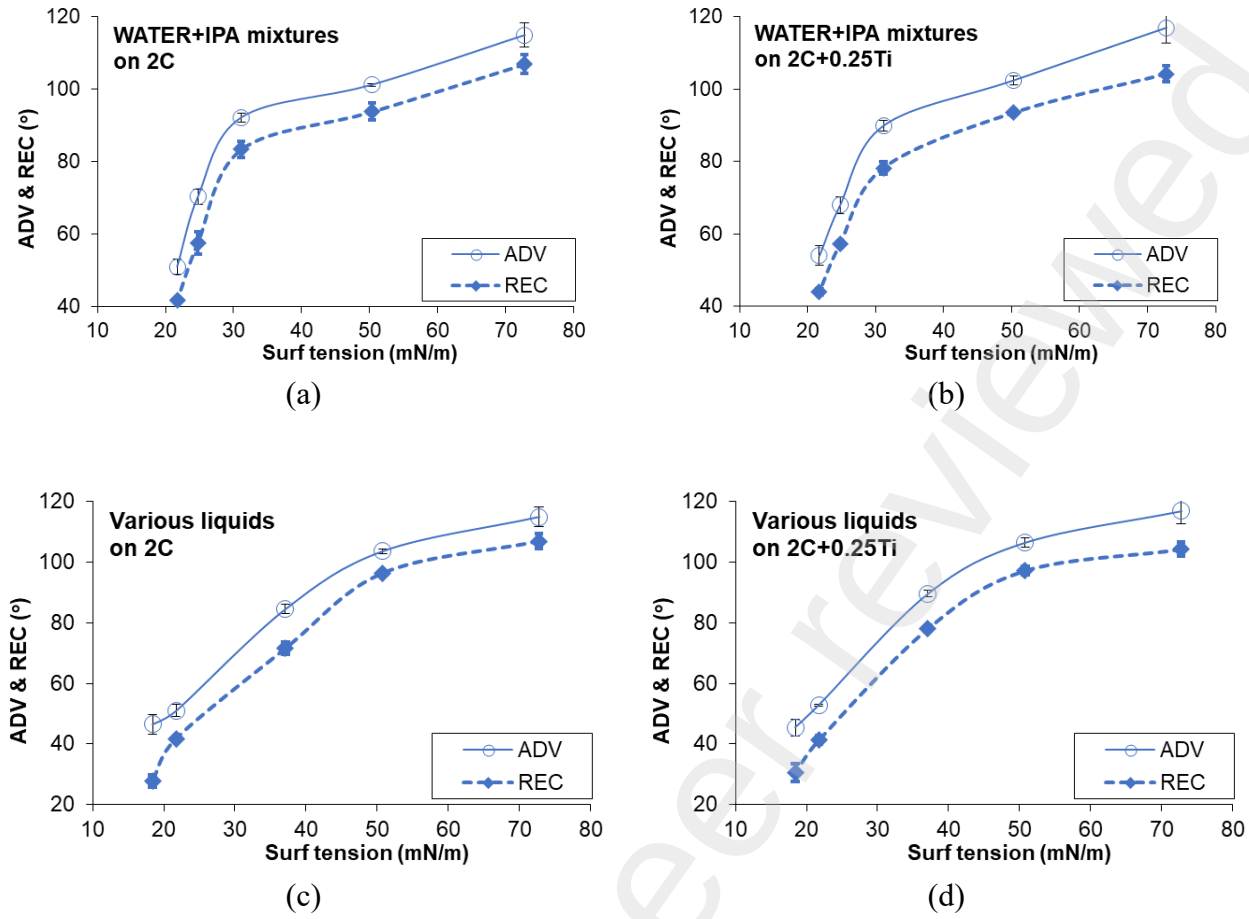

Figure S2. Advancing (ADV) and receding (REC) contact angles of (a) drops of water+IPA mixtures on 2C, (b) drops of water+IPA mixtures on 2C+0.25Ti, (c) drops of various liquids on 2C and (d) drops of various liquids on 2C+0.25Ti.

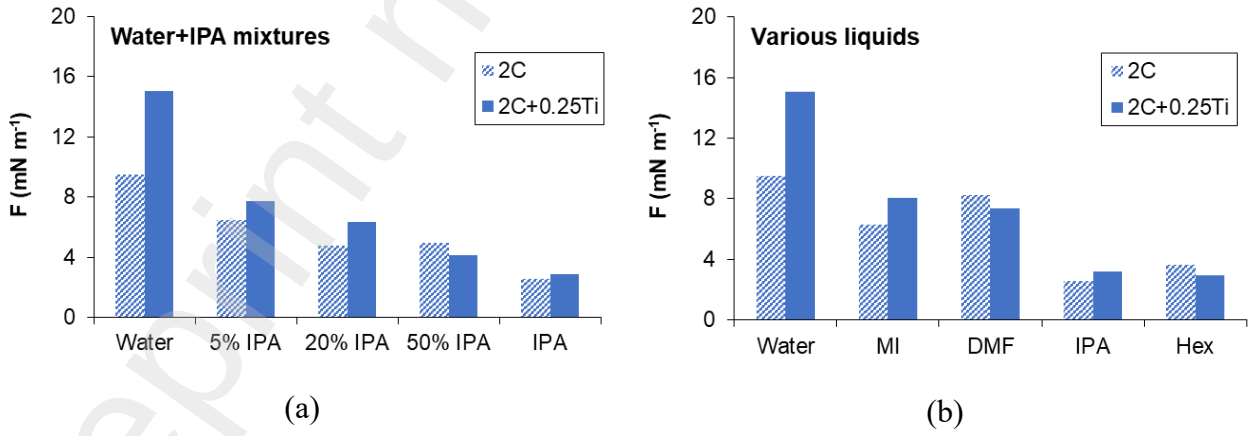

Figure S3. Advancing (ADV) and receding (REC) contact angles of (a) drops of water+IPA mixtures and (b) drops of various liquids, on 2C and 2C+0.25Ti. The tested liquids in (b) are water, diiodomethane (methylene iodide MI), N,N-dimethylformamide (DMF), isopropanol (IPA) and n-hexane (Hex).

Table S2. Dispersive (γ_L^d) and polar (γ_L^p) components of the surface free energy of the liquid (γ_L) for water and diiodomethane obtained from the literature[(c)].

Liquid	**γ_L^d (mN m^{-2})**	**γ_L^p (mN m^{-2})**	**γ_L (mN m^{-2})**
Water	21.8	51	72.8
Diiodomethane	49.5	1.3	50.8

[(c)]D.K. Owens, R.C. Wendt, Evaluation of the surface free energy of polymers, *J. Appl. Polym. Sci*. 13 (**1969**) 17411–1747.